Dual Inverter Configuration for Grid-Connected Photovoltaic Generation Systems

Gabriele Grandi, Darko Ostojic, Claudio Rossi
Alma Mater Studiorum - University of Bologna
Department of Electrical Engineering
Viale Risorgimento 2, 40136 - Bologna, Italy
[*gabriele.grandi, darko.ostojic, claudio.rossi*]*@mail.ing.unibo.it*

Abstract - **The design and control issues associated with the development of a novel three-phase grid-connected photovoltaic generation system are discussed in this paper. The scheme is based on two insulated strings of panels, each one feeding a standard two-level three-phase voltage source inverter (VSI). Inverters are connected to grid by a three-phase transformer with the open winding configuration on primary side. The resulting conversion structure performs as a multilevel power active filter, doubling the power capability of a single VSI with given current rating.**

An original control method has been introduced to regulate the dc-link voltages for each VSI. The proposed algorithm has been verified by numerical tests with reference to different operating conditions. The simulation results confirm the effectiveness of the whole conversion scheme.

I. Introduction

Photovoltaic (PV) panels produce electricity, while using no moving parts, consuming no fuel, and creating no pollution. Because of constantly growing energy demand, grid-connected photovoltaic systems are becoming more and more popular, and many countries have permitted, encouraged, and even funded distributed power generation systems. Yet the technology presents shortcomings such are high initial installation cost and low energy conversion efficiency, requiring constant improvement of both cell and power converter technology [1].

One of the classification criteria for PV systems is the way in which relatively low and weather-dependant voltage is "boosted" to reach grid voltage level. A series connection of adequate number of panels could seem as the simplest solution but it involves considerably large number of panels in series. Therefore the output current and performance of the system is constrained by the weakest cell, including partial shadowing or failure [2]. Remaining solutions are to include dc to dc converter stage, or transformer, or even both. In many countries national electric code requires transformer's presence to achieve galvanic insulation of panels with respect to the network. Even if topology includes transformer (either high- or line-frequency), the system with a dc/dc converter will operate over a wider input voltage range but with higher cost and lower conversion efficiencies at most operating points. Transformerless and high-frequency transformer are preferred for omitting bulky LF transformer and already commercially presented, but limited to single-phase output with powers up to few kW. The restrictions arise from switching losses and limited power of the HF magnetic components. Hence PV converter with line-frequency transformer is prevailing in higher power range, i.e., from few tens of kW up to 1000 kW, contributed by the fact that LF transformer's cost per watt decreases as rated power increases.

A novel topology for PV grid-connected systems is proposed in this paper. It utilizes dual inverter structure connected to open-end primary windings of a standard three-phase transformer. Each inverter can be directly coupled with the panels, or through dc/dc stage (denoted with dashed lines) - an option available for all PV converters [1]. The secondary windings are connected to the grid with traditional star configuration (Fig. 1). Note that the transformer contributes with its leakage inductance to the ac-link inductance which is always necessary for the grid connection of a VSI.

Advantage of the topology is simplified hardware structure with respect to traditional multilevel inverters, increasing both the effectiveness and the reliability in medium- and high-power applications. Also, it can use standard six-transistor configuration readily available also as modules, without additional diodes and switches. A control algorithm

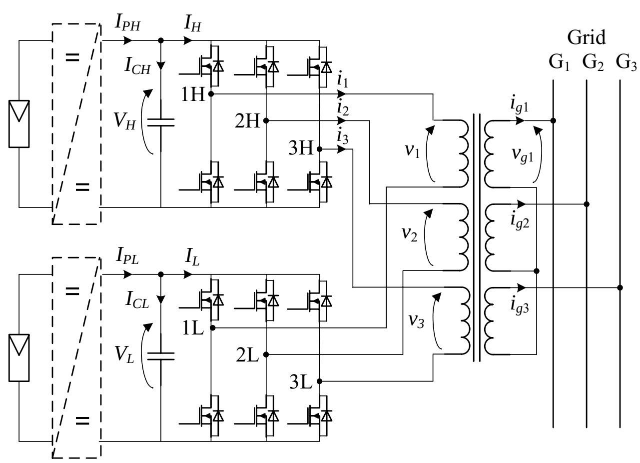

Fig. 1. Proposed dual-inverter configuration.

978-1-4244-1628-8/07/$25.00 ©2007 IEEE

with standard PI controllers is proposed to achieve commanded values of dc voltages necessary for maximum power point tracking (MPPT) of PV panels. Beside power generation the system can function as an “active filter”, with the additional capabilities of load balancing, harmonics compensation and reactive power injection. Complete analysis, together with numerical simulations, is presented for verifying system performance in the case of different variations of the solar irradiance and possible topologies (with and without dc/dc converter).

II. Dual Inverter Topology

In low voltage high power applications designer inevitably encounters the problem of high currents exceeding available switch's ratings. One common way to overcome this limitation is paralleling of more switches, but it brings drawbacks in current protection, circuitry complexity and current sharing. A viable solution to overcome this constraint is multilevel inverter. Among many proposed solutions, three-level converters are a good tradeoff solution between performance and cost in high-voltage and high-power systems [3]-[4]. The main advantages of three-level inverters are reduced voltage ratings for the switches, good harmonic spectrum (making possible the use of smaller and less expensive filters), and good dynamic response. In particular, the output voltage waveform of the conversion unit has a multilevel behavior, producing up to nine output levels of phase voltage. Since dual two-level inverter (Fig. 1) can give the same output voltage as three-level inverter, it makes more convenient solution. Another advantage is lack of voltage balance problems that occur in multi-level converters [5]. However, the control complexity increases compared to conventional VSI.

In comparison with standard three-phase inverter, the dual inverter achieves double rated power twice as much switches, therefore making overall switch utilization for two configurations equal. It can be said that the switches in those two cases are just repartitioned. The benefit lays in the fact that dual converter's output rated current is halved for the same rated power and voltage. Another benefit is the ability to produce up to nine output voltage levels versus only five of standard three-phase inverter, thus having output voltage less distorted. It makes easier to meet demands of the standards given by the utility companies regarding current harmonics with smaller passive filter components.

The presence of transformer enables choice of low dc voltage. In this case, only parallel connection of panels can be considered. The resulting PV array voltage is generally between 30-50 V, which allows use of low-voltage MOSFETs. These types of MOSFETs are widely used in automotive applications and they are very cheap semiconductor devices. Furthermore those components feature good efficiency, since their on-state resistance is a strong decreasing function of the blocking voltage rating. However, maximum power rating of converter using low PV array voltage is limited to few tens of kW. For higher powers the proposed topology can be utilized with higher dc side inverter’s voltage (400-700 V). Demanded dc voltage range can be directly obtained by increased PV array voltage with series connection of more panels. Another possibility is inclusion of dc/dc converter, which simultaneously takes over role of MPP tracker, enabling optimal and constant dc voltage for dual inverter. For even higher powers (above few hundred kW) converter can be directly connected to medium voltage level (10-20 kV).

Beside somewhat higher complexity, the main drawback in comparison to standard inverter configuration is the potential path for the zero sequence currents. If dual inverter is about to be supplied from single dc source, it requires implementation of component (reactor or transformer) with high zero-sequence impedance to suppress correspondent current flow. Both options mean higher cost and dimensions of the system. Another possible solution is application of voltage modulation algorithm which doesn’t produce zero sequence voltage, but this leads to lower utilization of available voltage by 15.5 % and thus higher costs of the system [6]. In some applications, such is PV, it is simple and convenient to separate panels in two strings since string subdivision is commonly accepted array topology. Although division prevents undesired zero sequence current from flowing, it should be noted that it requires two set of sensors (for each string) and makes control algorithm more complicated.

With reference to the scheme on Fig. 1, using space vector representation, the output voltage vector $\bar{v}$ of the multilevel converter is given by the contribution of the voltage vectors $\bar{v}_H$ and $\bar{v}_L$, generated by inverter H and L respectively [7]:

$$\bar{v} = \bar{v}_H + \bar{v}_L . \quad (1)$$

The combination of the eight switching configuration for each inverter yields total 64 switching states corresponding to 19 different output voltage vectors, including zero vector. The resulting hexagonal locus can be subdivided in two

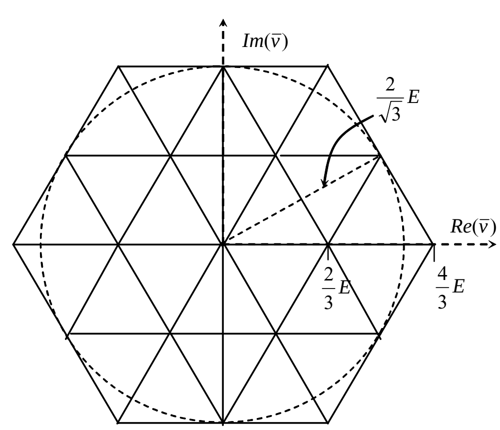

Fig. 2. Dual inverter voltage vector plot in the case $V_H = V_L = E$.

areas, as represented in Fig. 2: the inner hexagon and the outer belt [8]. In a grid-connected application voltage vector is always positioned in the outer belt, which means both inverters "H" and "L"' are contributing to the output voltage.

III. Inverter Control

The proposed system is symmetric having both inverters with equal ratings and two equal groups of panels supplying them. Nevertheless two distinct voltage controllers have to be implemented to compensate unavoidable mismatches, originating from cell production nonidealities or small differences in cleanness and/or position. The primary control task is voltage regulation of both PV arrays to accomplish MPP for both of them. In the following, the voltage control is described in more detail while the MPP and other necessary supervisory tasks of the system control are not discussed further. It is important to note that control task is much more complex than in case of a single inverter configuration, because the proposed system is multivariable. While in single inverter configuration the only variable being controlled is ac current, in case of dual inverter ac current but nonetheless inverter's output ac voltages sharing between "H" and "L" inverters is influencing the state of the system. In this paper a novel control algorithm based on simple PI controllers is proposed. The problem is somewhat similar to power sharing problem investigated in automotive applications, where proper multilevel voltage modulation strategy has been addressed [8]. In [9] the more complex approach of LQR techniques based on state-space models is considered, whereas in [10] an independent control of each inverter is proposed for integrated starter-alternator drive in automotive application.

The two dc voltages (V_H, V_L) are controlled by two proportional-integral controllers, giving as output the reference of two dc currents (I^*_H, I^*_L). A feed-forward action can be added in order to compensate sudden changes in PV currents (I_{PH}, I_{PL}), as shown in Fig. 3. Its utilization depends on the current transducer's availability and required response dynamic. The inverter output current reference is calculated based on the previous controllers references and power balance equation in steady-state.

$$V_H I_H + V_L I_L = 3V'_g I \, , \tag{2}$$

where V'_g is the grid voltage seen from the inverters' side (RMS) and I is inverters' ac output current (RMS). Note that in (2) both inverter and transformer losses are neglected. Thus, from (2) current reference can be obtained as

$$I^* = \frac{1}{3}\frac{V_H I_H^* + V_L I_L^*}{V'_g} \, . \tag{3}$$

The current injected into the grid is assumed to be in phase with grid voltage, i.e. having only active component. Nevertheless reactive or harmonic compensation current references can be added in a same manner, if required.

The inverter reference voltages $\bar{v}_H^*$, $\bar{v}_L^*$ are determined on the basis of the following equations

$$\bar{v}_H^* = \frac{I_H^*}{I_H^* + I_L^*}\bar{v}^* \, , \qquad \bar{v}_L^* = \frac{I_L^*}{I_H^* + I_L^*}\bar{v}^* \, . \tag{4}$$

Since inverters "H" and "L" have common output current, their share in total output power is determined by the ratio of voltages:

$$\frac{|\bar{v}_H|}{V'_g} = \frac{V_H I_H}{V_H I_H + V_L I_L} \, , \quad \frac{|\bar{v}_L|}{V'_g} = \frac{V_L I_L}{V_H I_H + V_L I_L} \tag{5}$$

Substituting (4) in (5) shows that ratio of the inverter's instantaneous powers is proportional to the ratio of their controller's outputs. This approach ensures a faster response of the system, since the controller with greater error has a sort of "priority".

The voltage drop across the total leakage inductance L determines the inverters' output current $\bar{i}$

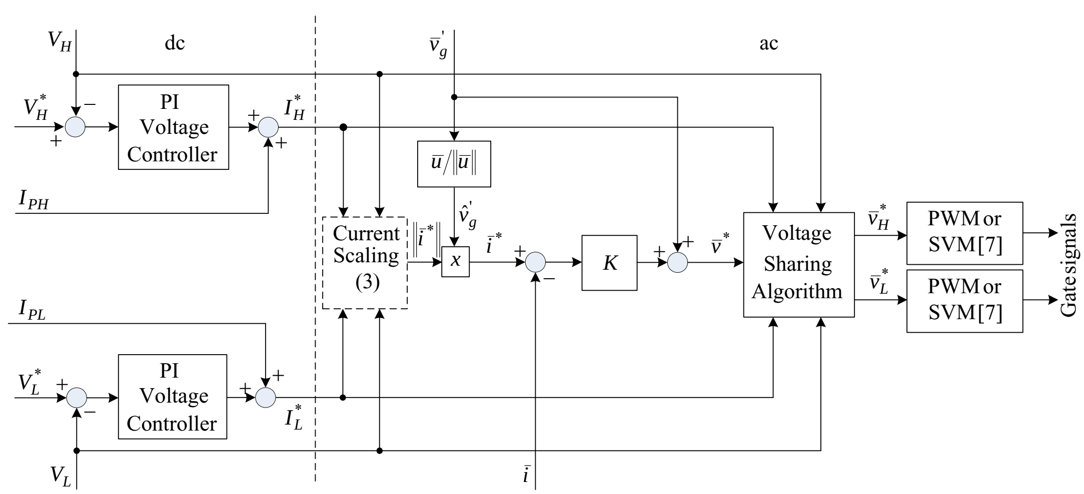

Fig. 3. Block diagram of proposed control system.

$$\bar{v} = L\frac{d\bar{i}}{dt} + \bar{v}'_g \,, \tag{6}$$

being $\bar{v}'_g$ the grid voltage seen from the inverters' side. Then, by neglecting the magnetizing current of the transformer, the current regulation can be achieved by a simple proportional controller, as follows

$$\bar{v}^* = K(\bar{i}^* - \bar{i}) + \bar{v}'_g \,. \tag{7}$$

Further, it has to be provided that both references are within range of achievable output voltage of particular inverter, which depends on their dc voltages. This is an issue on which this topology differs from case of a single inverter topology, where no problems arise when the voltage demand exceeds available dc voltage. Here total voltage reference must be satisfied, so in case of voltage saturation of one inverter the second has to make up the missing part. This is achieved by the voltage sharing algorithm shown in Fig. 4.

IV. System Implementation

The simulation model of the proposed topology and control scheme represented in Figs. 1 and 3 was implemented in MATLAB-Simulink, using *SimPowerSystems* library. The component ratings used for model are based on real laboratory equipment which will be used for future experimental tests. The PV panels have been electrically represented by the fitted I-V characteristic of a parallel arrangement of "*Solar Shell*" SP150 modules. The main characteristics of the PV generation system are summarized in Table I.

The value of the ac-link inductance is a tradeoff between acceptable current ripple and available dc voltage. Low inductance will give a high current ripple and will make a design more dependent on the line impedance. A high value of inductance will give a low current ripple, but simultaneously create a high voltage drop at line frequency and therefore reduce the operation range of system, increasing its cost and dimensions. Since the role of ac-link inductance is to filter output current, in that purposes could be utilized transformers leakage inductance, analogously to inverter drive applications where same role is performed by motor leakage inductance. Unfortunately, the leakage inductance of standard transformer is about two or three times lower that in a case of motor with same rated power. Hence, a modified transformer structure or an additional series inductor could be necessary to provide the required value of the ac-link inductance, especially in the case of low voltage windings.

Table I

System Prototype Characteristics

Quantity	Value	Quantity	Value
PV panel power (peak)	150 W	Line-to-line grid voltage	400 V, 50 Hz
Total PV power (peak)	1.2 kW	Transformer rated power	1.5 kVA
PV array connection (2 arrays)	4 in parallel	Transformer short-circuit voltage	5.6 %
PV array short-circuit current	20 A	dc link capacitance	2 mF
PV array no-load voltage	45 V	PWM carrier frequency	20 kHz

V. Simulation Results

In simulation tests reference is made to the different conversion system topologies depicted in Fig. 1, i.e., with and without the dc/dc choppers enclosed by dashed lines in Fig. 1. The first case is related to the case of a direct connection between the two PV arrays and the two inverters. In this case the MPPT regulation is achieved by the change of inverters' dc bus voltage. Note that a possible implementation of MPPT algorithm could be similar to the one proposed in [11] and also discussed in [12], where a small voltage displacement in the operating points of the two PV arrays is introduced to determine the actual slope of the $P(V)$ characteristic (i.e., the sign of dP/dV).

Figure 5 shows the time behavior of the dc voltages in case of sudden change of voltage reference, demanded by the MPPT control algorithm as a response to the change of solar irradiation. The change is chosen to be much faster than in real conditions, in order to test ability of the control system. It can be seen that the system response is very fast, and both voltage respond equally (their traces on figure are overlapping). In particular, the control parameters have been chosen to obtain a behavior similar to a critical damped response, with very slight overshoot. The output of the dual inverter during the whole executed simulation has been shown in Fig. 6. Particularly, zoom of the inverter output is shown in Fig. 7. The current is slightly lagging behind voltage because of the inductors and transformer reactive power demand. Grid

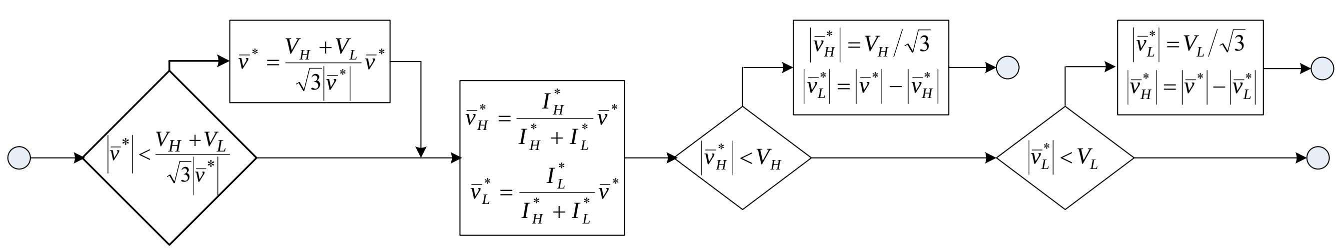

Fig. 4. Block diagram of proposed control system.

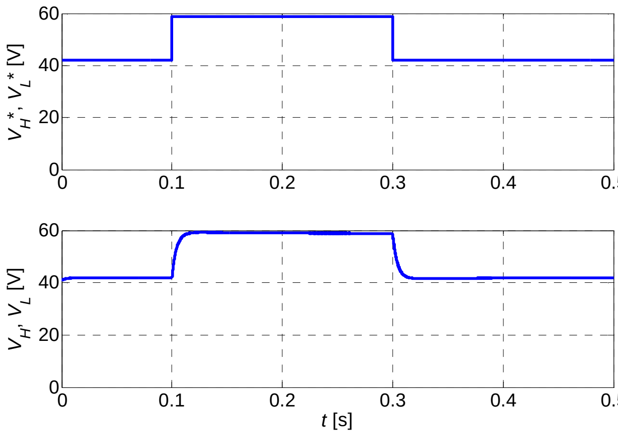

Fig. 5. Inverters dc voltage (lower trace) in the case of step change of the voltage reference (upper trace).

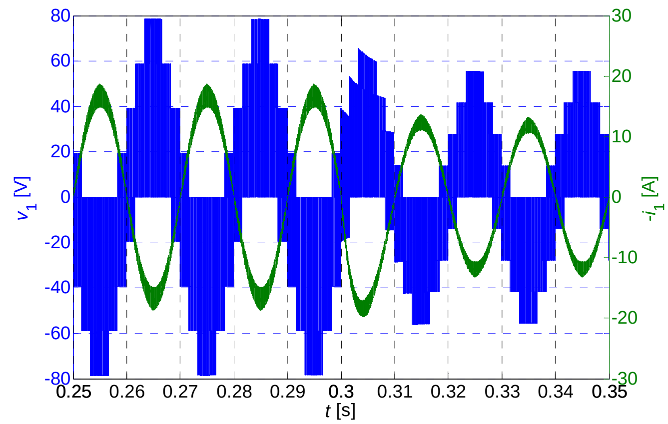

Fig. 7. Dual inverter output voltage and current (detail of Fig. 6).

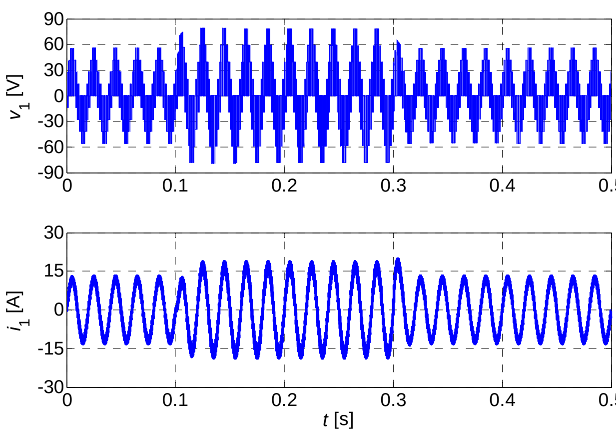

Fig. 6. Dual inverter output voltage and current.

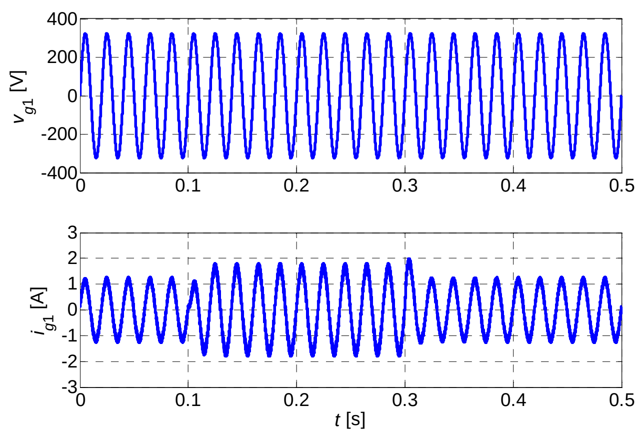

Fig. 8. Grid voltage and current

current and voltage are in phase, and current ripple is acceptable. The figure also shows that converter isn't achieved proper multilevel operation since transitions between non-adjacent voltage levels can be noticed. It is a consequence of the implemented control algorithm's simplicity. Similar output has been accomplished in [10]. In order to achieve multilevel behavior of converter system requires application of more detailed SVM algorithms, such is [7]. Since grid voltage is constant, the increase of power generation is followed by increase of current, as can be seen in Fig. 8. The phase-to-neutral voltage and the correspondent current are almost ideally in phase, as defined by control algorithm.

The second case investigated by simulations is related to the presence of dc/dc choppers between PV panels and the two inverters. In this case the MPPT regulation is implemented by the dc/dc choppers, and the dc bus voltage can be kept constant close to its optimal value. The choppers act as current sources with a current injection proportional to the solar irradiation. Figure 9 shows the time behavior of the dc bus voltages in case of sudden change of injected currents. The transient is chosen to be much faster than in real system, in order to test ability of the control system. Furthermore, the presented case includes high degree of asymmetry between sources, which is not so common in real conditions. It can be seen that the system response is very fast, and the corresponding perturbations on the dc bus voltages are small. The transients in one dc source are also affecting the other one, since the two inverters are coupled by the common output connection. Fig. 10 shows output of the dual inverter, whereas Fig. 11 is a zoomed detail on the output. Finally, Fig. 12 shows grid voltage (phase-to-line value) and current. As expected, those outputs are very similar to the one shown in the preceding simulation case.

VI. Conclusion

A novel conversion topology for the grid connection of a photovoltaic generation system is presented and discussed in this paper. The proposed power conditioner utilizes a dual inverter structure to extend rated maximum power on the basis on standard three-phase inverters. The topology includes two insulated PV arrays and a three-phase open-winding transformer. The resulting power conditioning system is able to behave as a multilevel inverter, with active filter capability.

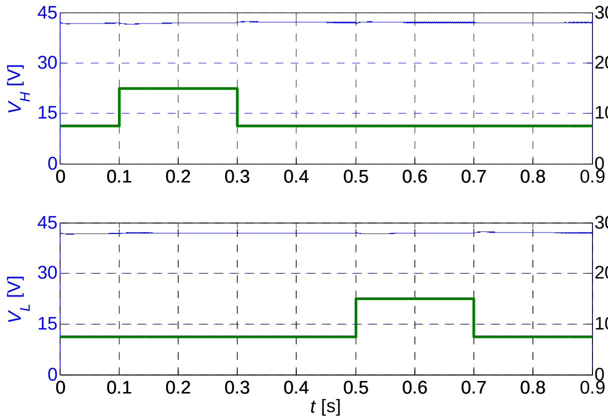

Fig. 9. Inverter dc voltage (upper traces) in the case of step change of PV current injection (lower traces).

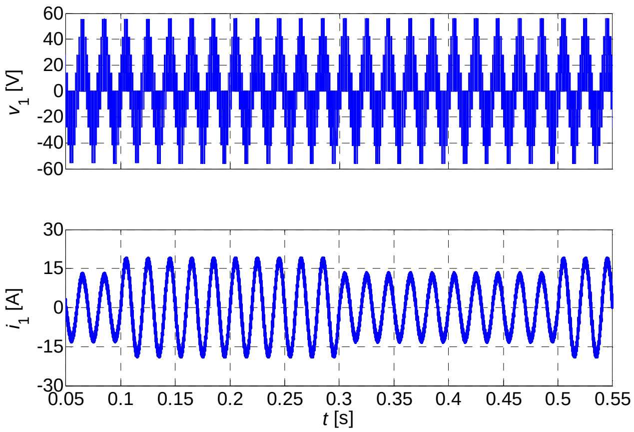

Fig. 10. Dual inverter output voltage and current.

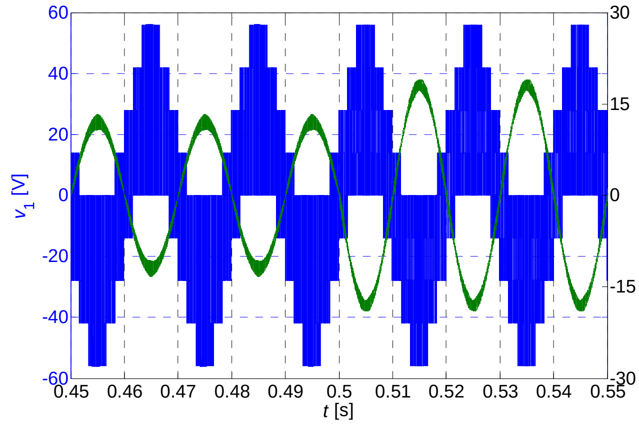

Fig. 11. Dual inverter output voltage and current (detail of Fig. 10).

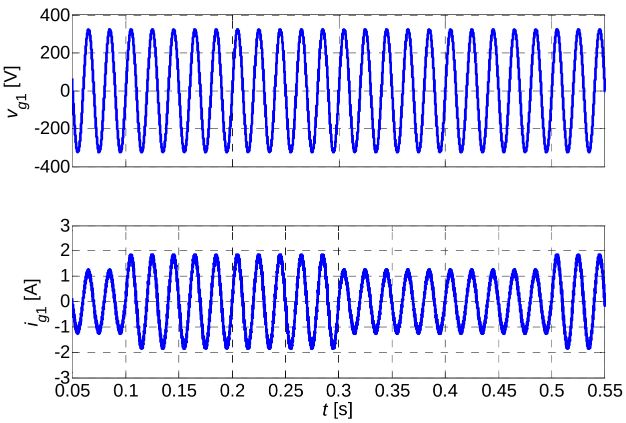

Fig. 12. Grid voltage and current.

A simple and effectiveness control algorithm is introduced for the system regulation. It is able to provide power generation with unity power factor and maximum power point tracking, even in case of two unbalanced strings.

The whole system has been preliminarily designed and tested by numerical simulations, showing good performance both in steady state and transient conditions.

References

[1] S. Kjaer, J. Pedersen, F. Blaabjerg: "A Review of Single-Phase Grid-Connected Inverters for Photovoltaic Modules", IEEE Trans. Ind. Applications, Vol. 41, No. 5, pp. 1292-1306, Sep 2005.

[2] T. Shimizu, M. Hirakata, T. Kamezawa, and H. Watanabe, "Generation control circuit for photovoltaic modules," IEEE Trans. on Power Electronics, Vol. 16, No. 3, pp. 293-300, May 2001.

[3] I. Takahashi and Y. Ohmori, "High-performance direct torque control of an induction motor," IEEE Trans. Ind. Appl., Mar. 1989, vol. 25, no. 2, pp. 257-264.

[4] Y. Kawabata, N. Yahata, M. Horii, E. Ejiogu, T. Kawabata, "SVG using open-winding transformer and two inverters," Proc. IEEE Power Electron. Spec. Conf. PESC, vol.4, pp. 3039- 3044, 2004.

[5] K. Corzine, A. S. Sudhoff, C. Whitcomb, "Performance characteristics of a cascaded two-level converter," IEEE Trans. on Energy Conversion, vol. 14, No. 3, pp. 433-439, Sep. 1999.

[6] M. Baiju, K. Mohapatra, R. Kanchan, K. Gopakumar, "A dual two-level inverter scheme with common mode voltage elimination for an induction motor drive," IEEE Trans. on Power Electron. vol. 19, No. 3, pp. 794-805. May 2004.

[7] G. Grandi, C. Rossi, A. Lega, D. Casadei, "Multilevel operation of a dual two-level inverter with power balancing capability," Proc. of IEEE Industry Applications Soc. Annual Meeting, IEEE-IAS, Tampa, Florida (USA), Oct. 8 - 12, 2006.

[8] G. Grandi, C. Rossi, A. Lega, D. Casadei, "Power balancing of a multilevel converter with two insulated supplies for three-phase six-wire loads," Proc. of 11th European Conference on Power Electronics and Applications, EPE 2005, Dresden (D), September 11-14, 2005.

[9] S. Alepuz, S. Busquets-Monge, J. Bordonau, J. Gago, D. Gonzalez, J. Balcells, "Interfacing Renewable Energy Sources to the Utility Grid Using a Three-Level Inverter," IEEE Trans. on Industrial Electronics, vol. 53, no. 5 pp. 1504-1511, Oct. 2006.

[10] J. Kim, J, Jung, K, Nam, "Dual-inverter control strategy for high-speed operation of EV induction motors," IEEE Trans. on Industrial Electronics, vol. 51, no. 2, Apr. 2004, pp. 312- 320.

[11] J.H. Park, J.Y. Ahn,, B.H. Cho, G.J. Yu, "Dual-module-based maximum power point tracking control of photovoltaic systems," IEEE Trans. on Industrial Electronics, Vol. 53, No. 4, June 2006, pp. 1036-1047.

[12] G. Grandi, C. Rossi, G. Fantini, "Modular Photovoltaic Generation Systems Based on a Dual-Panel MPPT Algorithm," Proc. of IEEE International Symposium on Industrial Electronics, IEEE-ISIE, Vigo (Spain), June 4-7, 2007.